Physics Letters A 376 (2012) 566–572

Contents lists available at SciVerse ScienceDirect

Physics Letters A

www.elsevier.com/locate/pla

Inverse freezing in the van Hemmen fermionic Ising spin glass with a transverse magnetic field

F.M. Zimmer [a,*], I.C. Berger [a], S.G. Magalhaes [b]

[a] Departamento de Fisica, Universidade Federal de Santa Maria, 97105-900 Santa Maria, RS, Brazil
[b] Instituto de Fisica, Universidade Federal Fluminense, 24210-346 Niterói, RJ, Brazil

ARTICLE INFO

Article history:
Received 23 August 2011
Received in revised form 13 October 2011
Accepted 25 October 2011
Available online 22 November 2011
Communicated by A.R. Bishop

Keywords:
Quantum spin glass
Fermionic model
Inverse freezing transition

ABSTRACT

The inverse freezing (IF) is studied with a quantum fermionic van Hemmen spin glass (SG) model. The disorder is treated without the use of replica method, in which an exact mean field solution is obtained for two different types of quenched disorders: the bimodal and the gaussian ones. The IF is then observed for certain range of chemical potential when the gaussian distribution is adopted. However, IF is destroyed by the quantum fluctuations. Particularly, the results suggest that the nontrivial SG free energy landscape, represented by strong disordered SG models, is not a necessary condition to generate a spontaneous IF.

1. Introduction

Inverse transitions, melting or freezing, are a class of counter-intuitive phase transitions in which an ordered phase appears at higher temperature than a disordered one. In other words, the ordered phase is more entropic than the disordered one. This kind of phase transition was already very well known in physical systems, as Rochelle salts [1,2] or liquid crystals [3,4]. However, more recently, there are increasing numbers of new physical systems which display inverse transitions. The interesting point is the wide variety of such systems. For instance, polymers [5], magnetic thin films [6], high temperature superconductors [7] and organic monolayers [8].

From the theoretical point of view, the understanding of what ingredients a model should have to display inverse transitions is a quite important issue. Schupper and Schnerb [9] suggested that there are two classical magnetic models which seem to contain these ingredients: the Blume–Capel (BC) [10] and the disordered Gathak–Sherrington (GS) [11] models. They are composed by three state spin variables with two competing mechanisms: (i) an interacting term favoring the magnetic states; (ii) an anisotropic term favoring the non-magnetic ones. These models have been studied with several techniques as the mean field approximation and Monte Carlo simulations [9,12–14]. The mean field investigation of BC model shows inverse melting from the paramagnetic (PM) phase to the ferromagnetic one, as the temperature increases; although, only if an additional degeneracy of the interacting states is artificially introduced [9]. In contrast, inverse freezing (IF) is found in the mean field study of the GS model by using the replica method. In other words, there is a first order transition from the PM phase to the spin glass (SG) phase as temperature increases [13]. Quite recently, results from Monte Carlo simulation for the disordered BC model, in which the spin–spin coupling J_{ij} is a random variable following a bimodal, has been investigated in three dimensions confirming the existence of IF [12]. Thus, this result suggests that besides a mechanism favoring magnetic states or non-magnetic ones in a certain model, the presence of strong disorder and frustration should also be a necessary ingredient to produce spontaneous IF. Particularly, these two last characteristics are related to the SG phase, which shows a nontrivial broken ergodicity that is characterized by a complicated free energy landscape with the existence of an infinite number of almost degenerated free energy valleys separated by huge barriers [15]. In this context, the question if this free energy landscape is also relevant to the existence of IF rises. Therefore, it is important to study another type of disordered model able to present IF. That is precisely the point investigated in the present work.

Other magnetic disordered models have been used [16–20]. An example is the infinite-range fermionic Ising spin glass (FISG) model, in which the spin operators are given in terms of fermionic operators. In this model, the chemical potential μ controls the site occupation and, eventually, can favor double occupation or empty sites. In fact, the FISG model displays IF in phase diagram temperature versus μ. It should be noticed that it would be expected since the FISG model and the GS one are quite connected [21,22]. In this sense, the FISG model is not able to add much new information on

* Corresponding author. Tel.: +55 055 3220 9521.
E-mail address: fabiozimmer@gmail.com (F.M. Zimmer).

0375-9601 © 2011 Elsevier B.V. Open access under the Elsevier OA license.
doi:10.1016/j.physleta.2011.10.061

the IF problem as compared to the GS model. However, the FISG model has been also studied in the presence of a transverse magnetic field Γ. In that case, the IF is suppressed. The mechanism is that the increase of Γ favors the half filling occupation [18]. As a conclusion, one could say that this study confirms that the favoring of the dilution (here defined as the presence of magnetic and non-magnetic states in a model) would be an important condition to a magnetic disordered model to display IF. There is another disordered model, the so-called Hopfield fermionic spin glass (HFISG) model [18,19], in which the spin coupling J_{ij} is given as Hopfield classical model [23] instead of the gaussian distribution used in the FISG model. Mostly important, in its mean field solution there is a parameter which allows to control the level of frustration in the problem. As a result, PM/SG reentrance is found as the level of frustration is increased. Therefore, one could say that this work suggests that the presence of frustration would be a condition to a certain model to present IF. However, this SG solution has still the same properties as that one of the FISG model. To put it in another way, the GS, FISG and HFISG models have been studied within a mean field solution by using the replica method which presents a clear interpretation for that complicated SG free energy landscape [15]. In addition the IF appears in a region of first order transition that can present some difficulties on picking out the correct SG solution. In this region, there is more than one SG solution, but all solutions are replica symmetric unstable. Even for the replica symmetry breaking (RSB) study, it is not obvious how to choose, among all the SG solutions, the one which satisfies the stability criterion. This situation can be a serious problem to locate the first order boundary phase and any possible reentrance. Furthermore, these SG models can also present stability problems associated with fluctuations on the replica diagonal elements that introduce negative and complex eigenvalues of the Hessian matrix (longitudinal eigenvalues) [21,24,25]. Therefore, it would be important to study the existence of IF in a model where the disorder and frustration could be treated without the use of the replica method.

In that sense, the van Hemmen (vH) model [26] can be very useful. This classical model has been originally introduced to investigate the SG problem as an alternative to the Sherrington–Kirkpatrick (SK) model [27] exactly because it is not necessary to use the replica method. Furthermore, the vH model solution lacks the intricate free energy landscape, but it attempts to several thermodynamic properties of SG systems [28]. Quite recently, a fermionic version of the vH model [29] has been proposed to investigate the SG phase in the presence of a Γ field with a great advantage. The absence of replica method simplifies the SG solution, which allows one to always choose a stable solution.

This work aims to study a fermionic version for the vH model in the presence of a transverse magnetic field, in which issues addressed to the existence of IF are investigated. Particularly, it attempts to answer the following questions: Is the complex free energy landscape with a large multiplicity of states a necessary condition for the IF occurrence? In other words, is the vH type of disordered interaction (with many spin states) able to produce spontaneously an IF transition? If the IF can be observed for the vH type of disorder, how is the IF affected by quantum spin flip fluctuations? For these purposes, the present quantum model considers magnetic dilution with non-magnetic sites (controlled by a chemical potential) and frustration generated by disordered vH interactions, which allows an exact mean field solution without using replicas. The fermionic path integral formalism is adopted to obtain the grand canonical potential, in which the order parameters are introduced within the static approximation [30]. The problem is analyzed for two types of quenched disorder: one given by a discrete bimodal random distribution and the other given by a continuous gaussian distribution.

This work is structured as follows. Section 2 introduces the model and the corresponding thermodynamics are calculated. Section 3 is dedicated to discuss the numerical results that are shown in phase diagrams of the temperature versus the ferromagnetic interactions and temperature versus μ for several ferromagnetic interactions and transverse fields. The entropy behavior versus the temperature is also discussed. These results are presented for the two different types of quenched disorder. Section 4 is holding to the conclusions.

2. Model

The fermionic van Hemmem (FvH) model with a magnetic transverse field Γ is described by

$$H = -\frac{2J_0}{N}\sum_{i\neq j}\hat{S}_i^z\hat{S}_j^z - 2\sum_{i\neq j}J_{ij}\hat{S}_i^z\hat{S}_j^z - 2\Gamma\sum_i \hat{S}_i^x \tag{1}$$

where the sums are over the N sites. The spin operators are defined in terms of fermion creation ($c_{i\sigma}^\dagger$) and annihilation ($c_{i\sigma}$) operators as

$$\hat{S}_i^z = \frac{1}{2}[\hat{n}_{i\uparrow} - \hat{n}_{i\downarrow}] \quad \text{and} \quad \hat{S}_i^x = \frac{1}{2}\left[c_{i\uparrow}^\dagger c_{i\downarrow} + c_{i\downarrow}^\dagger c_{i\uparrow}\right] \tag{2}$$

where $\hat{n}_{i\sigma} = c_{i\sigma}^\dagger c_{i\sigma}$ gives the number of fermions at site i with spin projection σ ($\uparrow$ or $\downarrow$). In Eq. (1), J_0 represents a direct ferromagnetic coupling and J_{ij} is the disordered coupling given by

$$J_{ij} = \frac{J}{N}[\xi_i\eta_j + \xi_j\eta_i], \tag{3}$$

where ξ_i and η_i are independent random variables with symmetric distribution around zero and variance one. Particularly, the present work is restricted to the study of two different probability distributions: the bimodal (discrete distribution) and the Gaussian (continuous distribution). These distributions are respectively expressed by

$$P(x_i) = \frac{1}{2}\left[\delta(x_i - 1) + \delta(x_i + 1)\right] \tag{4}$$

and

$$P(x_i) = \frac{1}{\sqrt{2\pi}}\exp\left[-x_i^2/2\right] \tag{5}$$

with $x_i = \xi_i$ or η_i. Both distributions introduce frustration in the problem [26], but the continuous one presents a larger number of different values of ferromagnetic and antiferromagnetic interactions J_{ij}, that can generate a nontrivial frustration.

The partition function is obtained within the grand canonical ensemble by using the Lagrangian path integral formalism. In this case, the spin operators are represented as bilinear combinations of Grassmann fields (ϕ^*, ϕ) [31]:

$$Z = \int D(\phi^*\phi)e^{\int_0^\beta d\tau\{\sum_{i,\sigma}\phi_{i\sigma}^*(\tau)[-\frac{\partial}{\partial\tau}+\mu]\phi_{i\sigma}(\tau) - H(\phi^*(\tau),\phi(\tau))\}} \tag{6}$$

where μ is the chemical potential and $\beta = 1/T$ (T is the temperature). In the thermodynamic limit, the first terms of the Hamiltonian can be written such as

$$Z = \int D(\phi^*\phi)\exp\left[\int_0^\beta d\tau\left\{A_\Gamma(\tau) + A_I(\tau,\xi,\eta)\right\}\right] \tag{7}$$

with

$$A_\Gamma(\tau)=\sum_{i,\sigma}\phi^*_{i\sigma}(\tau)\left[-\frac{\partial}{\partial\tau}+\mu\right]\phi_{i\sigma}(\tau)+\Gamma\sum_i S^x_i(\tau), \tag{8}$$

$$A_I(\tau,\xi,\eta)=\frac{J_0}{2N}\left[\sum_i S^z_i(\tau)\right]^2-\frac{J}{2N}\left[\sum_i \xi_i S^z_i(\tau)\right]^2 -\frac{J}{2N}\left[\sum_i \eta_i S^z_i(\tau)\right]^2+\frac{J}{2N}\left[\sum_i(\xi_i+\eta_i) S^z_i(\tau)\right]^2 \tag{9}$$

where $S^z_i(\tau)=\sum_\sigma s\phi^\dagger_{i\sigma}(\tau)\phi_{i\sigma}(\tau)$ ($s=+$ for $\sigma=\uparrow$ or $s=-$ for $\sigma=\downarrow$) and $S^x_i(\tau)=\sum_\sigma\phi^\dagger_{i\sigma}(\tau)\phi_{i-\sigma}(\tau)$. The quadratic terms in Eq. (9) can be linearized by using Hubbard–Stratonovich transformations. This procedure results in the following expression:

$$Z=\int Dm(\tau)\int Dq_3(\tau)\int Dq_1(\tau)\int Dq_2(\tau) \times\exp\left\{-\frac{N}{2}\int_0^\beta d\tau\left[J_0m^2(\tau)+Jq_3^2(\tau)-Jq_1^2(\tau)-Jq_2^2(\tau)\right] -\ln(\Lambda)\right\} \tag{10}$$

where

$$\Lambda=\int D(\phi^*\phi)\exp\int_0^\beta d\tau\left\{A_\Gamma(\tau)+\sum_i h_i(\xi,\eta)S^z_i(\tau)\right\} \tag{11}$$

with $h_i(\xi,\eta)=J_0m(\tau)+J(q_3(\tau)-q_1(\tau))\xi_i+J(q_3(\tau)-q_2(\tau))\eta_i$.

The functional integrals over $\{q_n(\tau)\}$ ($n=1,2$ and 3) and $m(\tau)$ in Eq. (10) can be solved by using the steepest descent method ($N\to\infty$), which gives

$$q_1(\tau)=\frac{1}{N}\sum_i\langle\xi_iS^z_i(\tau)\rangle,\qquad q_2(\tau)=\frac{1}{N}\sum_i\langle\eta_iS^z_i(\tau)\rangle,\quad\text{and}$$

$$m(\tau)=\frac{1}{N}\sum_i\langle S^z_i(\tau)\rangle \tag{12}$$

with $q_3=q_1+q_2$ and $\langle\cdots\rangle$ is the average over the effective problem, Eq. (11). Particularly, the static approximation is assumed here, in which $q_n=q_n(\tau)$ and $m=m(\tau)$.

The Fourier transform is used in Eq. (11). Then the functional integral over the Grassmann fields is evaluated, and the sum over the Matsubara's frequencies is performed following Ref. [32]. Finally, the grand canonical potential per site $\Omega=-\frac{1}{N\beta}\langle\langle\ln Z\rangle\rangle$ is given by

$$\beta\Omega=\frac{\beta J_0}{2}m^2+\beta Jq^2-\beta\mu-\langle\langle\ln 2K(\xi,\eta)\rangle\rangle \tag{13}$$

with

$$K(\xi,\eta)=\cosh(\beta\mu)+\cosh\beta\sqrt{\left[J_0m+J(\xi+\eta)q\right]^2+\Gamma^2} \tag{14}$$

where the order parameters are obtained by the saddle point equations in which $q=q_1=q_2$. The notation $\langle\langle\cdots\rangle\rangle$ represents the average over the random variables ξ and η that follow either the bimodal distribution (Eq. (4)) or the Gaussian one (Eq. (5)). The grand canonical potential is also expanded in powers of q and m in Appendix A, which allows to analyze the continuous phase transitions.

The other thermodynamic quantities can be derived from Ω. For instance, the entropy s and the average occupation number ν are obtained from $s=-\partial\Omega/\partial T$ and $\nu=-\partial\Omega/\partial\mu$.

3. Numerical results

The numerical solutions for the set of order parameter equations (q and m) and thermodynamic quantities are presented in this section. The results are shown in phase diagrams T/J versus μ/J (or J_0/J) for the two probability distributions and several values of J_0 and Γ. The entropy behavior and occupation number are also exhibited. The parameters T, J_0, μ and Γ are in units of J that, for numerical purposes, $J=1$.

Fig. 1 shows phase diagrams of temperature as a function of ferromagnetic coupling J_0 at the half-filling occupation ($\mu/J=0.00$) for bimodal (Fig. 1(a)) and gaussian (Fig. 1(b)) distributions. For both distributions, the paramagnetic (PM) phase ($q=0$ and $m=0$) is found at high temperatures. Lowering the temperature, the PM phase suffers a second order transition to the SG phase ($q>0$ and $m=0$) if J_0 is small enough or to the FE phase ($q=0$ and $m>0$) if J_0 is high. As discussed in Appendix A, these critical lines are the same for both distributions. However, the location of the first order phase boundaries can depend on the random distribution. For example, at intermediary values of J_0, there is also a discontinuous SG/FE phase transition, where the SG appears at higher temperatures than the FE order.[1] In this case, the positions of the SG/FE first order transitions are different for the two random distributions (compare Figs. 1(a) and 1(b)). In addition, the phase diagrams exhibit other important difference at low temperature for small values of J_0. For instance, a mixed phase (SG + FE) ($q>0$ and $m>0$) can emerge below the SG order for the bimodal distribution (see Fig. 1(a) for $\Gamma/J=0.00$). On the other hand, if the bimodal distribution is replaced by the gaussian one, there is no mixed phase, as it is shown in Fig. 1(b). It suggests that the ground state for the bimodal distribution presents mixed phase or FE order, while the gaussian distribution presents SG or FE phases. These phase diagrams with $\Gamma/J=0.00$ are in qualitative agreement with that one obtained with classical spin variables [26].

Moreover, when the Γ is turned on, the transition lines are decreased to lower temperatures as shown in Fig. 1 for $\Gamma/J=0.5$. Therefore, the Γ field decreases the transition lines towards a quantum critical point (see Appendix A). For example, the mixed phase already disappears for $\Gamma/J=0.5$ (see Fig. 1(a)). In particular, the result for the FvH model with bimodal distribution was recently discussed in Ref. [19] and they are reproduced here for a completeness.

In the following sections, the effects caused by statistical charge fluctuations ($\mu>0$) are separately discussed for both distributions when $\Gamma/J=0$. First, the results for the FvH model with bimodal distribution are presented and after, the results for the gaussian one. The quantum flip process is then discussed in another section, in which results for both disorders are compared for $\mu>0$ and $\Gamma>0$.

3.1. Results for the bimodal distribution with $\mu>0$ and $\Gamma=0$

Fig. 2 presents phase diagrams T/J versus μ/J for the bimodal distribution and $\Gamma/J=0.00$ with $J_0/J=0.00$ (Fig. 2(a)) and $J_0/J=0.90$ (Fig. 2(b)). These results show that the behavior of the phase boundaries is affected by increasing the chemical potential μ. For example, in Fig. 2(a), the PM/SG second-order transition is gradually decreased by μ until a tricritical point (see Appendix A), where a PM/SG first-order take place. Therefore, the chemical potential introduces strong charge fluctuations that can cause changes in the nature of the PM/SG phase boundary. In ad-

[1] In the region of discontinuity, the stable solution is always that one of minimum Ω and the first order transition is located when Ω of the different phases become equal.

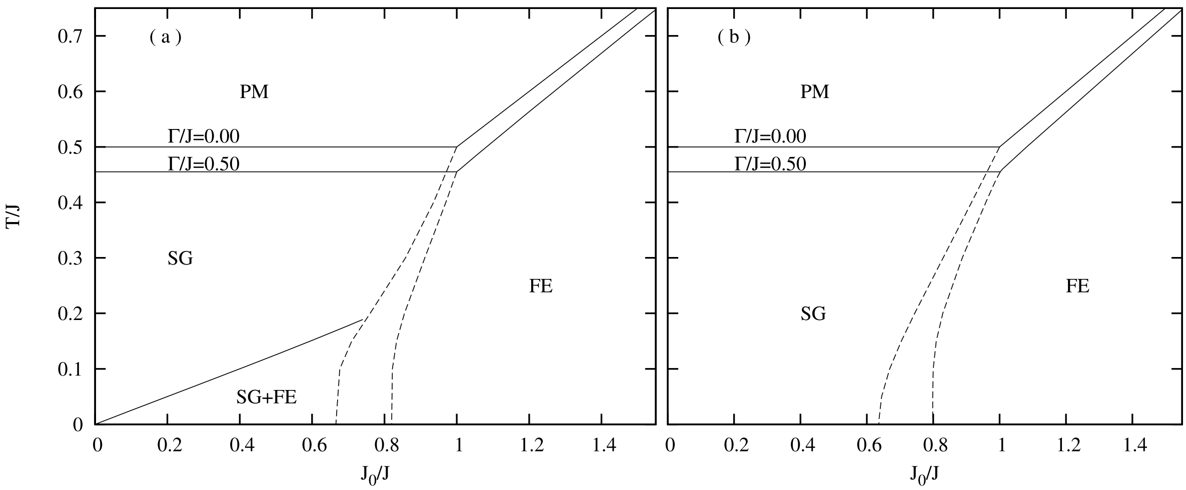

Fig. 1. Phase diagrams T/J versus J_0/J for $\mu/J = 0$ with two values of Γ/J: 0 and 0.5. The solid and dashed lines represent second and first order transitions respectively. Panels (a) and (b) show phase diagrams for the bimodal and gaussian distributions respectively.

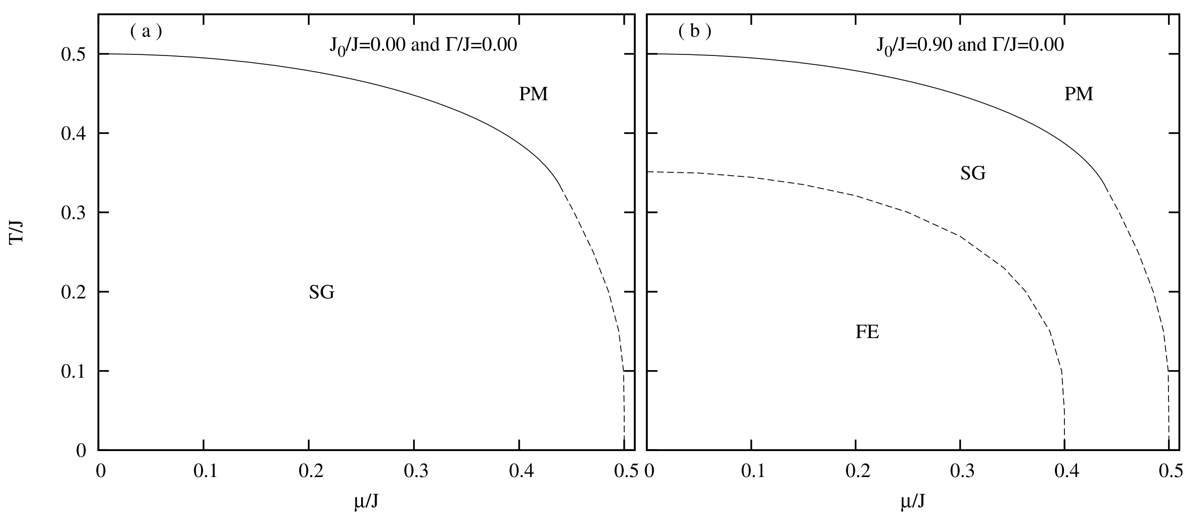

Fig. 2. Phase diagrams T/J versus μ/J for the bimodal distribution, $\Gamma/J = 0$ and two values of J_0. Results for $J_0/J = 0.00$ and $J_0/J = 0.90$ are presented in panels (a) and (b) respectively. Here the same convention lines as in Fig. 1 is used.

dition, when J_0/J increases to 0.90 (see Fig. 2(b)), the PM/SG still presents the same behavior as in the case of $J_0/J = 0.00$. However, a SG/FE first order transition at low temperature rises, which is also gradually suppressed by μ. For $J_0/J > 1.0$, the FE order becomes dominant at low temperature as pointed in Fig. 1(a) for $\mu/J = 0$, in which a PM/FE second order transition appears at a critical temperature T_c. The phase diagram T/J versus μ/J for this situation are not present here, but the behavior of T_c is such as T_c decreases as μ increases and a PM/FE first order transition occurs at large values of μ.

3.2. Results for the gaussian distribution with $\mu > 0$ and $\Gamma = 0$

Phase diagrams T/J versus μ/J for the Gaussian distribution and $\Gamma/J = 0.00$ are exhibited in Fig. 3. In this case, the PM/SG second order transition is decreased until a tricricical point when μ increases. As pointed in Appendix A, the behavior of the PM/SG second order transition is the same for both distributions. However, the PM/SG first order transition presents a remarkable change. Different from the bimodal distribution, in the gaussian distribution, the PM/SG first order region exhibits a reentrant transition that is associated with IF as discussed below. In other words, there is a range of μ in which the SG phase is obtained by increasing the temperature from the PM phase. This result is displayed in Figs. 3(a) and 3(b) for $J_0/J = 0.00$ and 0.90 respectively. Furthermore, the FE phase can be favored when J_0/J increases as it is shown in Fig. 1(b). For example, the FE region in the phase diagram T/J versus μ/J is enhanced by J_0/J, but the increase of μ still destroys the magnetic phases (see Fig. 3(b) for $J_0/J = 0.80$ (inset) and $J_0/J = 0.90$). Particularly, for J_0/J high enough, a complex phase diagram T/J versus μ/J can rise with the presence of a triple point. In addition, a PM/FE first order transition can also appear as it is exhibited in Fig. 3(b) for $J_0/J = 0.90$. Nevertheless, there is an important difference between the behavior of the PM/SG and the PM/FE phase boundaries. The first one can present a reentrant transition, while the second one has not been exhibited it at least in the present treatment. On the other hand, when the bimodal distribution is adopted, the FE order is destroyed before the SG phase as μ increases for the same value of J_0. Consequently, the complex scenario described above for the phase diagram T/J versus μ/J is not observed when the discrete distribution is used (see Fig. 2).

The entropy s, as a temperature function, is shown in Fig. 4(a) for $J_0/J = 0.00$ and two values of Γ. The behavior of s when $\Gamma = 0.00$ (solid line) is presented for $\mu/J = 0.43$ where the reentrance is found at $T/J = 0.10$ (see Fig. 3(a)). In this case, the

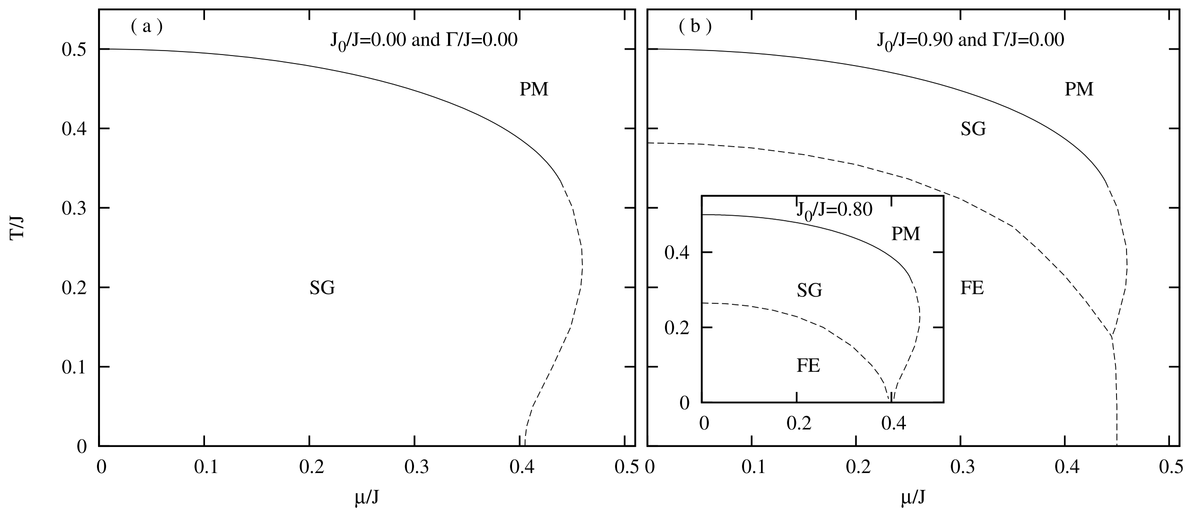

Fig. 3. Phase diagrams T/J versus μ/J for $\Gamma/J = 0$ and gaussian distribution. Panels (a) and (b) exhibit results for $J_0/J = 0.00$ and $J_0/J = 0.90$, respectively. The inset in panel (b) presents results for $J_0/J = 0.80$. The solid and dashed lines represent second and first order transitions respectively.

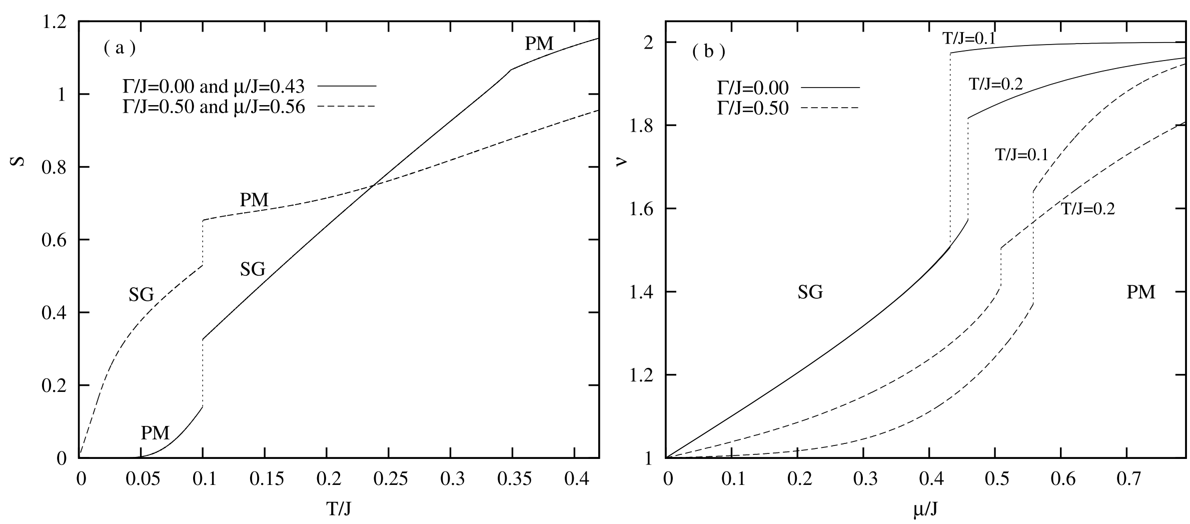

Fig. 4. (a) Entropy as a function of temperature for the gaussian distribution with $J_0/J = 0$, $\Gamma/J = 0.00$ and $\Gamma/J = 0.50$. (b) ν versus μ/J for two isotherms, $J_0/J = 0$, $\Gamma/J = 0.00$ and $\Gamma/J = 0.50$.

entropy of the PM phase at high temperature is higher than the SG one. However, the PM phase at low temperature exhibits lower entropy than the SG one. It means that an inversion of the standard order relation between the entropic contents of the PM and SG phases appears what characterizes the existence of IF. Therefore, the PM/SG reentrant transition for the gaussian distribution describes an IF.

The behavior of the average occupation number per site ν is exhibited in Fig. 4(b) for two isotherms ($T/J = 0.1$ and 0.2), $J_0/J = 0$, $\Gamma/J = 0.0$ (solid lines) and $\Gamma/J = 0.5$ (dashed lines). Particularly, the increase of μ favors the magnetic dilution with nonmagnetic sites (empty and double occupied sites). For example, the IF appears in a region where the PM phase presents high values of ν at low temperature. In this situation, the double occupation becomes dominant in the PM phase, which can be the cause of its low entropic value.

3.3. *Results for $\Gamma > 0$*

The entire transition lines are affected by Γ as illustrated in Fig. 5 that exhibits phase diagrams T/J versus μ/J for both distributions when $\Gamma/J = 0.50$ with $J_0/J = 0.00$ (Fig. 5(a)) and $J_0/J = 0.90$ (Fig. 5(b)). For example, the PM/SG transition is decreased with the location of the tricritical point changing to lower temperature and higher chemical potential when results for $\Gamma = 0.00$ (Figs. 2 and 3) are compared to that one for $\Gamma = 0.50$ (Fig. 5). The discontinuous transitions are also modified by Γ. In the case of the gaussian distribution, the reentrant transition is changed such as it is reduced until it is completely destroyed by the quantum fluctuations (see dashed lines of Fig. 5(a) for $\Gamma/J = 0.30$ (inset) and $\Gamma/J = 0.50$). Furthermore, the entropy curve for $\Gamma/J = 0.50$ shows that the IF disappears when Γ is high enough (see dashed line in Fig. 4(a)). In addition, the average occupation is also affected by Γ that redistributes charges decreasing the magnetic dilution (see dashed line in Fig. 4(b)). Therefore, the IF can be destroyed by quantum fluctuations.

4. Conclusions

The present work has studied the IF phenomenon by adopting a fermionic formulation for the van Hemmen SG model in the presence of a Γ field. This quantum SG problem allows an ana-

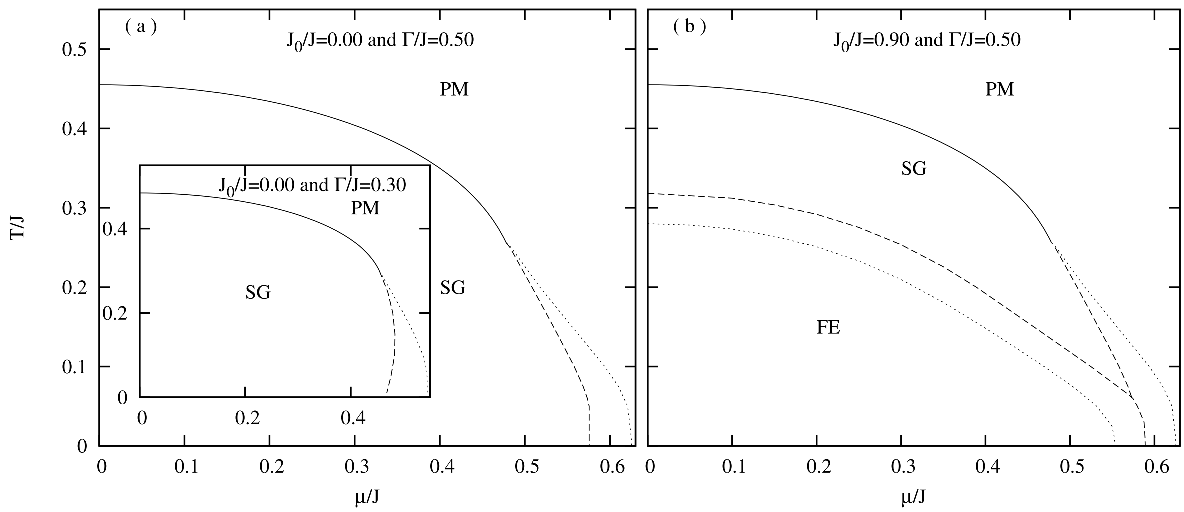

Fig. 5. Phase diagrams T/J versus μ/J when $\Gamma/J = 0.50$ for both distributions. Panels (a) and (b) exhibit results for $J_0/J = 0.00$ and $J_0/J = 0.90$, respectively. The dotted and dashed lines represent first order transitions for the bimodal and gaussian distributions respectively. The inset in panel (a) presents results for $J_0/J = 0.00$ and $\Gamma/J = 0.3$.

lytical treatment, in which the partition function is evaluated in the fermionic path integral formalism. An exact mean-field SG solution is then obtained without using the replica method, in which the grand canonical potential is analyzed for two different disordered interactions: one given by the bimodal distribution and the other one by the gaussian distribution.

The results are basically analyzed in phase diagrams of temperature versus direct ferromagnetic interactions J_0 and temperature versus chemical potential μ. They show that the SG phase can be found for small J_0, while the FE order is dominant at higher J_0. The chemical potential introduces statistical charge fluctuations that decrease the critical temperatures towards a tricritical point. In other words, the increase of μ favors the double occupation of sites causing a magnetic dilution. Particularly, the locations of the PM/SG and PM/FE second order transition lines and the thermodynamic properties of FE and PM phases are independent of the probability distribution. However, SG phase properties are strongly dependent on the disorder. For example, a mixed phase (SG + FE) can be obtained below the SG phase at lower temperatures when the bimodal distribution is adopted. This phase is absent for the disorder produced by the Gaussian distribution. This fact suggests that the quantity of frustrated interactions generated by the disorder obtained with the continuous distribution is higher than the discrete one when J_0 is weak. In addition, the SG/PM and SG/FE first order transitions depend on the particular disorder. In this case there is an important difference in the location of the SG/PM first order transition, which can present reentrance for the gaussian distribution. In other words, the PM/SG transition presents an IF for a range of μ when the bimodal distribution is replaced by the gaussian one. The increases of J_0 can also introduce a discontinuous FM/PM transition in phase diagrams of the temperature versus μ but without reentrance. On the other hand, the quantum spin flipping processes introduced by Γ affect the critical temperatures decreasing them to a quantum critical point. This quantum mechanism also destroys the IF observed when gaussian distribution is adopted.

Finally, the results suggest that the combined effect of frustration and magnetic dilution are really relevant to generate spontaneously IF, while quantum spin flipping destroys IF. Particularly, the present vH SG solution suggests that the complicated free energy landscape, with a large number of local minimum of free energy functional as observed in the stronger disordered SK type of interactions, is not a necessary condition to the spontaneous existence of IF. However, there is a critical level of frustration to observe spontaneous IF as pointed by comparing the present results for the bimodal and Gaussian distributions.

Acknowledgements

The authors gratefully acknowledge the support of the Brazilian agency CNPq. F.M.Z. also acknowledges the agency FAPERGS.

Appendix A. Landau expansion

The critical temperatures can also be investigated by using a Landau expansion for the grand canonical potential in powers of the order parameters q and m, which is given by

$$\beta\Omega = a_0 + a_2 q^2 + \frac{x\beta^2 J^4 A}{\Gamma^2 K_0} q^4 + b_2 m^2 + \frac{\beta^2 J_0^4 A}{8\Gamma^2 K_0} m^4, \tag{A.1}$$

where $a_0 = -\beta\mu - \ln(2K_0)$,

$$a_2 = \beta J\left(1 - \frac{J\sinh\beta\Gamma}{\Gamma K_0}\right), \tag{A.2}$$

$$A = -\cosh\beta\Gamma + \frac{\sinh\beta\Gamma}{\beta\Gamma} + \frac{\sinh^2\beta\Gamma}{K_0}, \tag{A.3}$$

$$b_2 = \frac{\beta J_0}{2}\left(1 - \frac{J_0\sinh\beta\Gamma}{\Gamma K_0}\right) \tag{A.4}$$

with $K_0 = \cosh\beta\mu + \cosh\beta\Gamma$ and $x = 1$ for the bimodal distribution or $x = 3/2$ for the gaussian distribution. Therefore, the expression (A.1) can be used for the two distributions studied here.

The second order transition from the PM to the SG phase (FM order) is obtained when $a_2 = 0$ ($b_2 = 0$) with $A > 0$. The tricritical points occur when $a_2 = 0$ and $A = 0$ (PM/SG transition) or $b_2 = 0$ and $A = 0$ (PM/FE transition). Therefore, the PM/SG and the PM/FE second order phase boundaries are the same for both distributions. For instance, when $\Gamma/J = 0$, the PM/SG line can be obtained from the relation $\mu/J = T/J\cosh^{-1}(T/J - 1)$, in which is considered that $T/J \geqslant T_{tr}/J = 1/3$ (T_{tr} is the tricritical temperature) and $J_0/J < 1$. In addition, if $\mu/J = 0$, the PM/SG critical temperature as a function of Γ is given by $T/J = \Gamma/J\frac{1}{\sinh^{-1}(2\Gamma/(J-\Gamma^2/J))}$ with the quantum critical point located at $\Gamma/J = 1$.

References

[1] F. Jona, G. Shirane, Ferroeletric Crystals, Pergamon, New York, 1962.
[2] B. Zeks, G.C. Shukla, R. Blinc, Phys. Rev. B 3 (1971) 2306.
[3] P.E. Cladis, R.K. Bogardus, W.B. Daniels, G.N. Taylor, Phys. Rev. Lett. 39 (1977) 720.
[4] P.E. Cladis, D. Guillon, F.R. Bouchet, P.L. Finn, Phys. Rev. A 23 (1981) 2594.
[5] S. Rastogi, G.W.H. Hohne, A. Keller, Macromolecules 32 (1999) 8897;
N.J.L. van Ruth, S. Rastogi, Macromolecules 37 (2004) 8191.
[6] O. Portmann, A. Vaterlaus, D. Pescia, Nature 422 (2001) 701.
[7] N. Avraham, B. Khaykovich, Y. Myasoedev, M. Rapoport, H. Shtrikman, D.E. Feldman, T. Tamegai, P.H. Kes, M. Li, M. Konczykowski, K. van der Beek, E. Zeldov, Nature 411 (2001) 451.
[8] A. Scholl, et al., Science 329 (2010) 303.
[9] N. Schupper, N.M. Shnerb, Phys. Rev. E 72 (2005) 046107.
[10] M. Blume, Phys. Rev. 141 (1966) 517;
H.W. Capel, Physica 32 (1966) 966.
[11] S.K. Ghatak, D. Sherrington, J. Phys. C 10 (1977) 3149.
[12] M. Paoluzzi, L. Leuzzi, A. Crisanti, Phys. Rev. Lett. 104 (2010) 120602;
L. Leuzzi, M. Paoluzzi, A. Crisanti, Phys. Rev. B 83 (2011) 014107.
[13] A. Crisanti, L. Leuzzi, Phys. Rev. Lett. 95 (2005) 087201.
[14] F.A. da Costa, Phys. Rev. B 82 (2010) 052402.
[15] K.H. Fischer, J.A. Hertz, Spin Glasses, Cambridge Univ. Press, Cambridge, 1991.
[16] F.M. Zimmer, C.F. Silva, C.V. Morais, S.G. Magalhães, J. Stat. Mech. 2011 (2011) 05026.
[17] S.G. Magalhães, C.V. Morais, F.M. Zimmer, Phys. Rev. B 81 (2010) 014207.
[18] S.G. Magalhães, C.V. Morais, F.M. Zimmer, Phys. Rev. B 77 (2008) 134422.
[19] C.V. Morais, F.M. Zimmer, S. G Magalhães, Phys. Lett. A 375 (2011) 689.
[20] C.K. Thomas, H.G. Katzgraber, arXiv:1104.2582v1, 2011.
[21] H. Feldmann, R. Oppermann, J. Phys. A 33 (2000) 1325.
[22] I.P. Castillo, D. Sherrington, Phys. Rev. B 72 (2005) 104427.
[23] D.J. Amit, Modeling Brain Function: The World of Attractor Neural Networks, Cambridge Univ. Press, Cambridge, 1989.
[24] S.G. Magalhaes, F.M. Zimmer, C.V. Morais, Physica A 388 (2009) 2140.
[25] F.A. da Costa, C.S.O. Yokoi, S.R.A. Salinas, J. Phys. A 27 (1994) 3365.
[26] J.L. van Hemmen, Phys. Rev. Lett. 49 (1982) 409;
J.L. van Hemmen, A.C.D. van Enter, J. Cqnisius, Z. Phys. B – Condensed Matter 50 (1983) 311.
[27] S. Kirkpatrick, D. Sherrington, Phys. Rev. B 17 (1978) 4384.
[28] J.L. van Hemmen, J. Phys. C: Solid State Phys. 19 (1986) L379.
[29] S.G. Magalhaes, F.M. Zimmer, C.V. Morais, Phys. Lett. A 374 (2010) 3354.
[30] A.J. Bray, M.A. Moore, J. Phys. C 13 (1980) L655.
[31] J.W. Negele, H. Orland, Quantum Many-Particle Systems, Addison–Wesley Publishing Company, USA, 1988.
[32] A. Theumann, A.A. Schmidt, S.G. Magalhaes, Physica A 311 (2002) 498.